A Versatile Window Function for Linear Ion Drift Memristor Model – A New Approach

Article *in* AEU - International Journal of Electronics and Communications · April 2018

DOI: 10.1016/j.aeue.2018.04.020

CITATIONS
23

READS
414

2 authors:

Anusudha t a
VIT University
3 PUBLICATIONS **24** CITATIONS
SEE PROFILE

S. R. S. Prabaharan
Inventus BioEnergy (P) Ltd
103 PUBLICATIONS **2,476** CITATIONS
SEE PROFILE

Regular paper (Yes, this article is registered as a regular paper. It is correct.)

A versatile window function for linear ion drift memristor model – A new approach

T.A. Anusudha (Surname is T. A. Given name is Anusudha)

S.R.S. Prabaharan (No, Surname is S. R. S. Given name is Prabaharan) (aran)*

prabaharan.srs@vit.ac.in (please add corresponding email as srsprabaharan1611@gmail.com as well) (corresponding author e-mail address is srsprabaharan1611@gmail.com)

School of Electronics Engineering, Vellore Institute of Technology, Chennai, Vandalur-Kelambakkam Road, Chennai 600127, Tamil Nadu, India

*Corresponding author (Please also add the corresponding author's private mail srsprabaharan1611@gmail.com).

Abstract

The memristor is a nano-scaled resistive switching device which is widely used investigated in analog and digital applications. We report here our success in formulating a new window function as applicable to linear ion drift model. Accordingly, this paper identifies the demerits of other existing window functions and the requirement of a versatile window function to mimic the current-voltage characteristics of a physical memristor device. The proposed new window function overcomes the demerits of existing window functions such as boundary effect, boundary lock (with respect to frequency of operation), and the scalability. The main significance of proposed model is to facilitate the nonlinearity in linear ion drift memristor model that produces the pinched hysteresis loop (a signature of a memristor) for any typical applied voltage within the frequency range ($0.05 \leq f < 2$ Hz). The validation of which has been verified in a memristor based op-amp circuitry. It exhibits a high gain compared to other existing models and produces low power dissipation compared to CMOS based op-amp.

Keywords: Memristor; Boundary effect; Boundary lock; Pinched hysteresis loop; Scalability; Window function

1 Introduction

Memristor is a missing fourth fundamental passive circuit element which is conceived by Leon Chua in 1971 [1]. Memristive device based on TiO_2 was apparently first demonstrated by Dmitri B. Strukov et al. [2]. Considering the resistive properties of memristor, it has become an element of surprise for various analog applications such as chaotic circuit, oscillators, filters, programmable analog circuit, sensors, cellular neural networks and alike [3–5] as well as digital applications viz., fuzzy processor [6] and non-volatile memory devices [4,5]. To throw more insight into memristors, various models have been proposed in the past focusing on obtaining Pinched Hysteresis Loop (PHL), a typical indicator of memristive characteristics. Hitherto, modeling of memristor is being carried out by using Linear Ion Drift Memristor Model (LIMM) [2], Non-Linear Ion Drift Memristor Model [7], Simmon Tunnel Barrier Model [8] and Team Model [9].

Each of these models has its own pros and cons. In LIMM, nonlinearity is very less and assumes two conditions which are (i) uniform electric field and (ii) the average mobility of ions [13]. To mitigate this problem, window functions play an important role in LIMM such as Jogelker [10], Biolek [11], and Prodromakis [12]. In view of various setbacks in using these revealed models with respect to LIMM, we introduce a new window function which overcomes the boundary lock issues pertaining to low frequency which was not thought of before according to our best knowledge. Accordingly, we have proven the versatility of our window function and compared its performance with respect to other existing window functions with respect to LIMM.

2 Linear ion drift memristor model

Memristor is defined as the rate of change of flux with respect to charge [1], which is represented in Eq. (1)

$$d\phi = M(q)dq \tag{1}$$

where $M(q)$ is the memristance.

The memristor consists of a bilayer of titanium-di-oxide which is sandwiched between two platinum electrodes [2,13] as shown in Fig. 1. The bilayer consists of two layers, one is oxygen deficient titanium-di-oxide (TiO_{2-x}) layer, which offers On State Resistance (R_{ON}) and another is perfect titanium-di-oxide layer (TiO_2) which offers Off State Resistance (R_{OFF}).

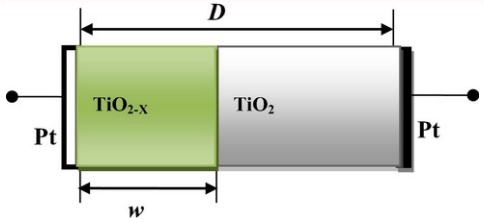

Fig. 1 Schematic structure of a bilayer memristor.

In memristor, the initial state of the memristance is high, which is shown in Fig. 2(a). When the positive voltage is applied across the memristor, the positively charged oxygen vacancies are drifted from TiO_{2-x} to TiO_2.Hence, the width of the defected titanium-di-oxide increases, simultaneously total memristance decreases and current conductivity increases. Therefore, the memristor switches from OFF state to ON state, which is illustrated in Fig. 2(b). This process is termed as the completion of growth of the conducting filaments [14]. At this stage the polarity is reversed, that is the negative voltage is applied at the Top Electrode (TE) with respect to the Bottom Electrode (BE), the positively charged oxygen vacancies are repelled from TiO_2 to $TiO_{2-x,}$ the process is termed as rupturing of the conducting filament [14]. As a result, the width of the defected titanium-di-oxide decreases consequently affecting the total memristance to increase and the current decreases. Thus, the memristor switches from ON state to OFF state as illustrated in Fig. 2(c).

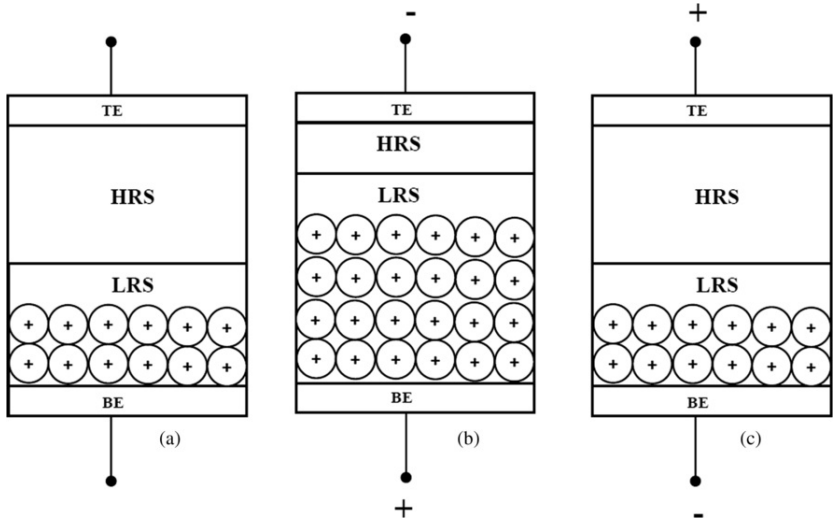

Fig. 2 Different bias conditions of a memristor (a) Before bias (b) Positive bias and (c) Negative bias.

The above said behavior is mathematically described in Eq. (2) for a linear ion drift memristor model,

$$V(t) = \left(R_{ON}\frac{w(t)}{D} + R_{OFF}\left(1 - \frac{w(t)}{D}\right)\right) I(t) \quad \textbf{(2)}$$

where $w(t)$ is the width of the non-stoichiometric region, $V(t)$ is the applied voltage, $I(t)$ is the current flow through the memristor, and D is the distance between the two platinum electrodes.

The LIMM is simulated in Cadence® software with virtuoso tool for the applied voltage of ±2 V at 0.5 Hz. It produces the bow-tie like loop the so-called PHL with less nonlinearity as shown in Fig. 3. In LIMM, it is understood that boundary effect and boundary lock are the two main prevailing problems. When the virtual boundary reaches to the metal/oxide interface, the rate of change of width (dw/dt) is suppressed to zero. Consequently, the memristance is fixed to either of the resistance states. That is, it is fixed either at minimum on-state resistance or maximum off-state resistance. This effect is known as boundary effect. On the other hand, if the applied voltage is large enough, then internal state variable (x) might reach the terminal boundaries faster and fixed at the boundary (+) as stated before. This phenomenon is known as boundary lock.

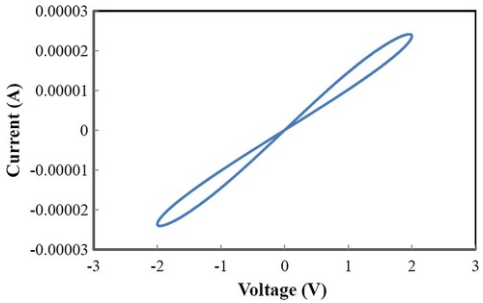

Fig. 3 The pinched *I-V* loop obtained for linear ion drift memristor model, a characteristic signature of a bilayer memristor.

3 Different types of window functions

Window functions are used to retain the ions within the boundaries and mimic the properties of the physical memristor device. By computing the parameters of the available window functions, it is possible to use memristor model in different electronic applications.

3.1 Jogelker window function

The Jogelker window function [10] is represented in Eq. (3)

$$f(x) = 1 - (2x - 1)^{2p} \tag{3}$$

where $f(x)$ represents the window function, p is the positive integer and x is the internal state variable.

3.1.1 Effect of p

In this model, $f(x)$ value does not scale up and scale down for the various value of p. Hence, the nonlinear *I-V* curves remain the same as shown in Fig. 4.

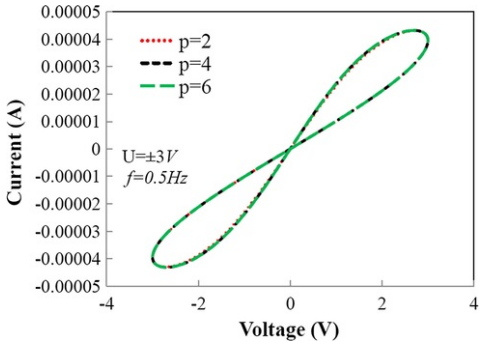

Fig. 4 Effect of p on nonlinear *I-V* curves (Jogelker window function).

When p value is large enough, then inverted parabolic curve of $f(x)$ is changed into a rectangular curve as shown in Fig. 5. Hence, this model provides a linkage with linear ion drift memristor model without window function.

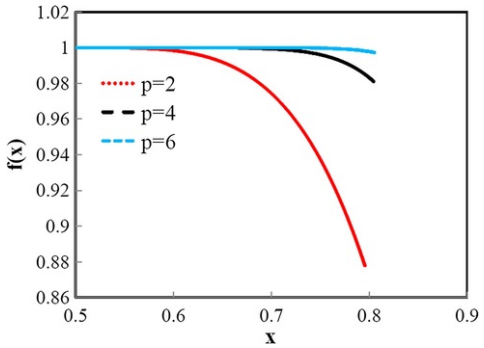

Fig. 5 Response of $f(x)$ vs x, for various values of p with the same parameters are used in Fig. 3.

3.1.2 Effect of applied voltage (U)

When an applied voltage increases, the amount of charges stored in the width of the non-stoichiometric region increases. Therefore, the nonlinearity of the memristor model increases as shown in Fig. 6. But, if the applied voltage is large enough, then model fails to retain the x within the interval $(0 < x < 1)$ as shown in Fig. 7. Therefore, this model fails to produce the PHL.

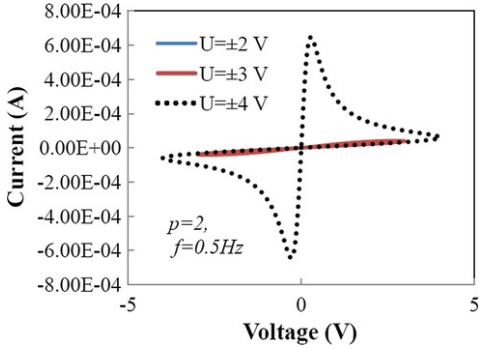

Fig. 6 *I-V* characteristic for various applied voltage (U) (Jogelker window function).

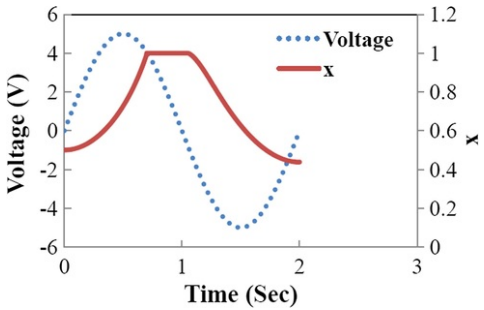

Fig. 7 Response of x, for $U = \pm 5$ V, $p = 2$, and $f = 0.5$ Hz (Jogelker window function).

3.2 Biolek window function

Biolek [11] resolves the problems of Jogelker window function with high nonlinearity and scalability.

The Biolek window function [2] is represented in Eq. (4).

$$f(x) = 1 - (x - stp(-i))^{2p} \quad (4)$$

$$stp(i) = \begin{cases} 1 & i \geq 0 \\ 0 & i < 0 \end{cases} \quad (5)$$

where p is the positive integer, and $stp(-i)$ is the step current flow through the memristor device, which is represented in Eq. (5).

3.2.1 Effect of p

In Biolek, the size of the nonlinear I-V curve is changed for the various value of p as shown in Fig. 8. It occurs due to $f(x)$ value being scaled up and scaled down for the various values of p, unlike Jogelker. This model provides the better scalability because it retains the $f(x)$ value within the range ($0 < f(x) < 1$). But, if the value of p is large enough, then model provides a linkage with LIMM without window functions.

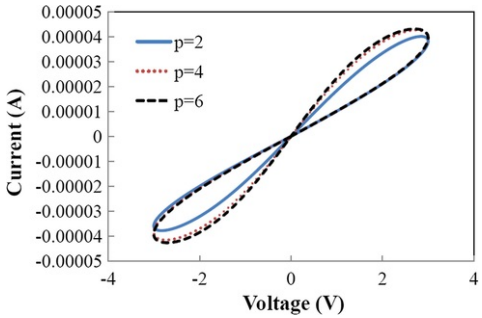

Fig. 8 PHL for the various value of p and fixed value of $U = \pm 3$ V, and $f = 0.5$ Hz (Biolek window function).

3.2.2 Effect of applied voltage (U)

A family of I-V curves is obtained for various applied voltages and particular p as shown in Fig. 9(a). Here, the nonlinear dopant kinetic is high due to introducing the step current in the window function, unlike Jogelker. But, this model fails to retain the PHL for high applied voltages ($U \geq \pm 6$ V) as shown Fig. 9(b). Because, the Biolek window function does not have a control parameter to control the x within the limited range of 0 and 1.

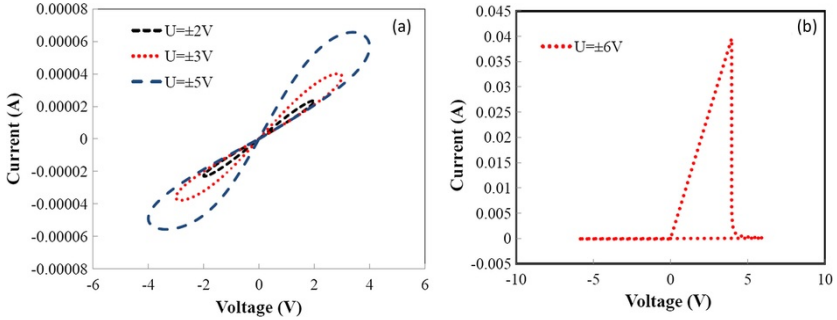

Fig. 9 PHL for different applied voltages and fixed value of $p = 2$, $U = \pm 2$ V, and $f = 0.5$ Hz (a) PHL (b) Distorted Pinched Hysteresis Loop (DPHL) for $U = \pm 6$ V (Biolek window function).

3.3 Prodromakis window function

The Prodromakis window function [12] is expressed in Eq. (6) which overcame the problems of Biolek with improved nonlinearity and scalability. The most significant function of this window is retaining the PHL for $f(x) \geq 1$.

$$f(x) = J(1 - [(x - 0.5)^2 + 0.75]^p) \quad (6)$$

where p and J are the control parameters.

3.3.1 Effect of p and J

The both p and J are the control parameters, which are used to control $f(x) < 1$ and $f(x) \geq 1$ respectively. This model retains the nonlinearity with high scalability for the large value of p unlike other window functions as shown in Fig. 10. Because, $f(x)$ value lies within the range $(0 < f(x) < 1)$ and if the value of p is large enough, then this model also provides a linkage with LIMM without any window functions.

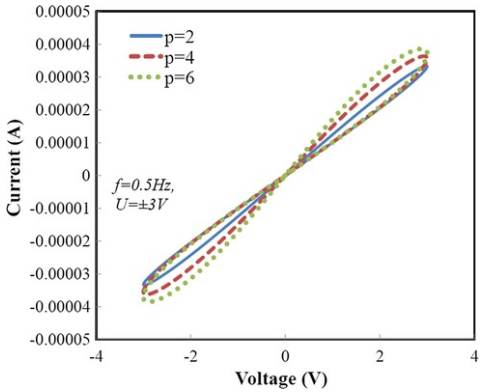

Fig. 10 Current-voltage response of the model for different value of p (Prodromakis window function).

Nevertheless, the factor J in Prodromakis window function plays an important role in increasing the nonlinearity as shown in Fig. 11. If the applied voltage is large enough then factor J controls the x within the range $(0 < x < 1)$ and produces the large size PHL with high nonlinearity. The main function of J is scaled up and scaled down the $f(x)$ and produces the PHL for $f(x) \geq 1$. Therefore, this model can be used in any memristor device applications with better performances.

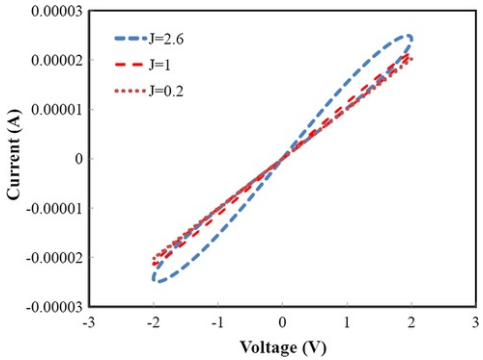

Fig. 11 Nonlinear I-V curves for fixed $U = \pm 2$ V, $f = 0.5$ Hz, and various J (Prodromakis window function).

3.3.2 Effect of applied voltage (U) and frequency (f)

A family of I-V curves is obtained for the applied voltages of ±2 V, ±4 V, ±6 V, ±8 V as shown in Fig. 12. This model retains the PHL up to the voltage of ±*10* V for frequency of 0.5 Hz, and distance between the two platinum electrodes of *3* nm. Therefore, the capacity of retaining the nonlinearity is high compared to the previous models. However, this model fails to retain the PHL for the frequency (f) < 0.1 Hz, and applied voltages of ±2 V due to x reaching the boundaries much faster leading to distorted PHL. Therefore, the flexibility of this model is reduced as illustrated in Fig. 19(c) for the frequency of 0.05 Hz.

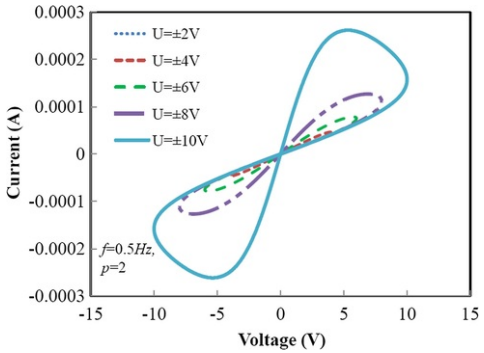

Fig. 12 Current-voltage for various applied voltages (Prodromakis window function).

3.4 Jinxiang window function

Jinxiang et al., window function [15] is expressed in Eq. (7) which is capable of addressing the aforementioned issues.

$$f(x) = J(1 - [0.25(x - stp(-i))^2 + 0.75]^p) \quad \textbf{(7)}$$

where p is the positive real number, J is the scaling parameter.

3.4.1 Effect of p and J

The Jinxiang et al., window function provides a high nonlinearity and scalability for the different value of p as shown in Fig. 13. It should be noted that the window function retains the $f(x)$ value within the range of 0 to 1. In addition, when value of p is large enough the model provides a linkage with LIMM without a window function. On the other hand, the J factor controls the x within the limited range of 0 to 1 and scale up/down the $f(x)$ from its maximum value of 1.

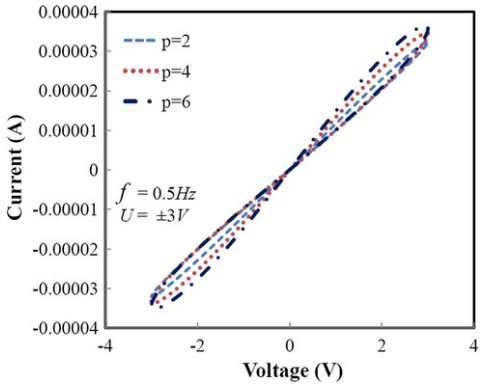

Fig. 13 Current-voltage response of the model for different value of p (Jinxiang et al., window function).

3.4.2 Effect of applied voltage (U) and frequency (f)

The model retains the PHL for $p = 2$, $J = 1$, $f = 0.5\ Hz$ and limited range of input voltages($\pm 2\,\text{V} \le U \le \pm 17\,\text{V}$). When the input voltage is (U) ≥ 18 V, the $f(x)$ value does not remain at one. Therefore, the model produces DPHL as shown in Fig. 14.As a result, this model fails to retain the high nonlinearity. On the other hand, ~~their~~ this model also fails to retain the PHL for the frequency (f) of 0.05 Hz, and the applied voltage of ±2 V due to x reaching the boundaries much faster leading to distorted PHL which is also illustrated in Fig. 19(d).

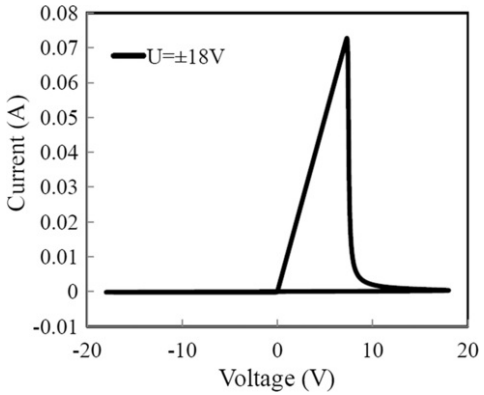

Fig. 14 The current-voltage response of the model for input voltage (U) ≥ ±18 V (Jinxiang et al., window function).

3.5 Proposed window function

Keep the above stated setbacks in the existing window functions; we have proposed and defined a new window function by considering the cubic parabola as given in Eq. (8).

$$f(x) = J[1 - 2(x^3 - x + 1)^p] \quad \textbf{(8)}$$

where $f(x)$ is the window function, x is the internal state variable, p is the positive integer, and J is the control parameter.

Due to this consideration in our window function, for any value of p, $f(x)$ value does not fix to any integer constant and lies within the interval $(0 < f(x) < 1)$. Thus, we have successfully overcome the problems of Jogelker, Biolek, Prodromakis and Jinxiang et al., window functions with high performances. The following validation ensures the success of this new proposed window function.

3.5.1 Effect of p and J

Interestingly, for any value of p, our new model incorporating the proposed window function transforms the linear ion drift model into nonlinear ion drift memristor model producing the large size PHL as shown in Fig. 15. The reason being is that $f(x)$ is controlled by the p factor and more importantly it does not fix to any particular integer constant as a Jogelker window function. Therefore, it increases the scalability significantly.

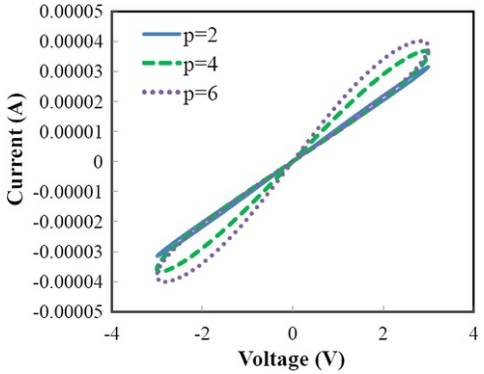

Fig. 15 Response of our model for the different value of p with the input voltage $U = \pm 3$ V, $f = 0.5$ Hz (proposed window function).

Fig. 16 exhibits the effect of our model which produces the PHL with diminished DNDR (Dynamic Negative Differential Resistance) for higher applied voltage (as high as ±50 V). On the other hand, one can also achieve a symmetric PHL by controlling the J factor. Obviously, the J factor plays an important role in controlling the x within the range from 0 to 1.

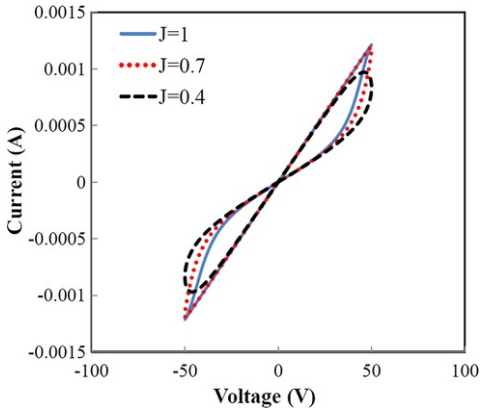

Fig. 16 Symmetric PHL, for the input voltage $U = \pm 50$ V, $p = 2$, and $J = 0.4$ (proposed window function).

3.5.2 Effect of applied voltage (U)

The proposed model retains the large size symmetric PHL for the voltage range $\pm 2\ \text{V} \leqslant U \leqslant \pm 26\ \text{V}$ as shown in Fig. 17. Because $f(x)$ value lies within the range $(0 < f(x) < 1)$ consequently, x lies within the interval $(0 < x < 1)$ as shown in Fig. 18. Therefore, our proposed model is found to overcome the setbacks enunciated by the Prodromakis and Jinxiang et al., window function. Even though the applied voltage is $(U) > \pm 26$, our proposed model produces the PHL with diminished DNDR, unlike other window functions as shown in Fig. 16.

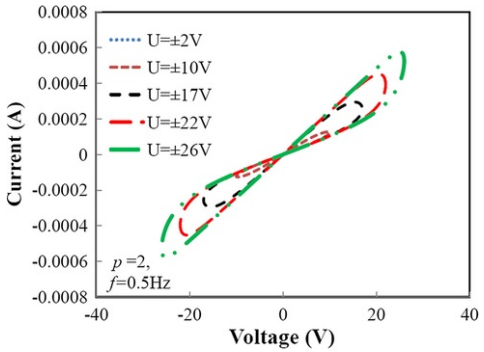

Fig. 17 Current-voltage response of the proposed model with the various input voltages (U) (proposed window function).

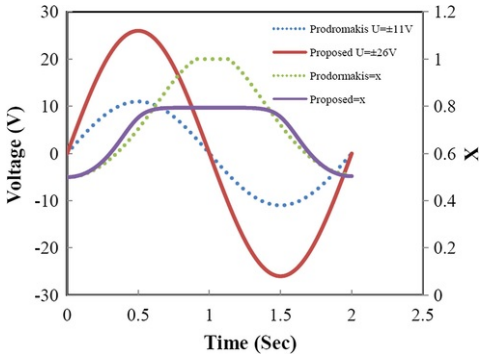

Fig. 18 The state variable response of the Proposed and Prodromakis window functions.

Generally, if the applied voltage is high, the rate at which the changes in the width is much faster facilitating the depleted ions to reach the boundary (metal electrode interface) causing DPHL to occur. This problem is eradicated by our proposed window function by controlling the rate of width movement yet retaining the x within the range ($0 < x < 1$).

3.5.3 Effect of frequency (f)

In general, memristor models produce linear *I-V* curve for high frequencies as it has direct relation to changing width with respect to ion mobility. This limits the charge (q) accumulation in the width of the non-stoichiometric region. Similarly, when the frequency decreases, the charges reach the boundary quickly consequently x reaches the boundaries with high speed as well. Therefore, the memristor model produces the Distorted Pinched Hysteresis Loop (DPHL).

Interestingly, these issues are resolved by using our proposed model. Thus, our proposed model produces the PHL within the frequency range $0.05 \leq f < 2$ Hz as illustrated in Fig. 20 unlike other window functions as depicted in Fig. 19. It is noteworthy that the new window function controls the width within the boundaries. On the other hand, by using the optimal values of p and J, our model produces the PHL for $f \geq 2$ Hz as shown in Fig. 21.

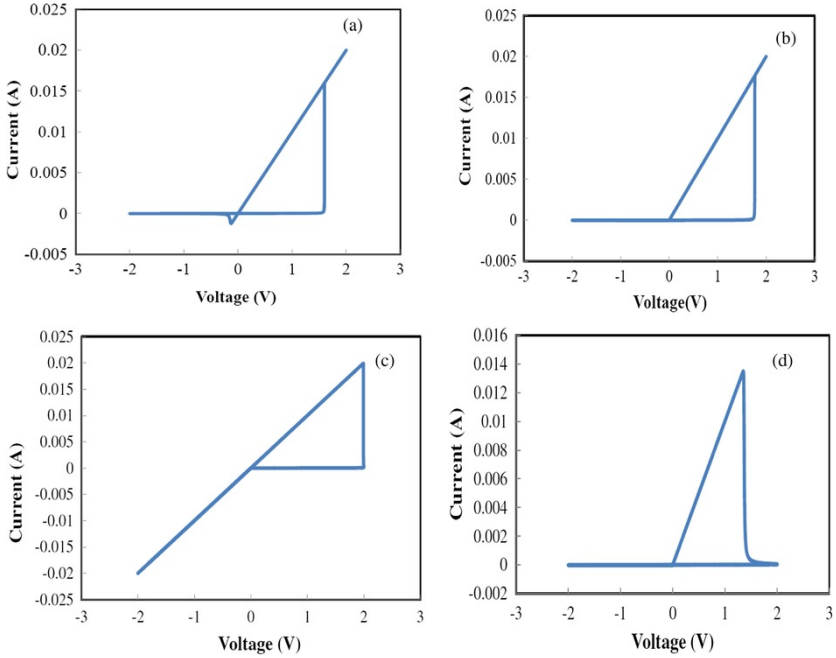

Fig. 19 The nonlinear *I-V* characteristics for the frequency $f = 0.05$ Hz, $p = 2$, $U = \pm 2$ V and, $J = 1$ (a) Jogelker, b) Biolek, (c) Prodromakis, and (d) Jinxiang window functions.

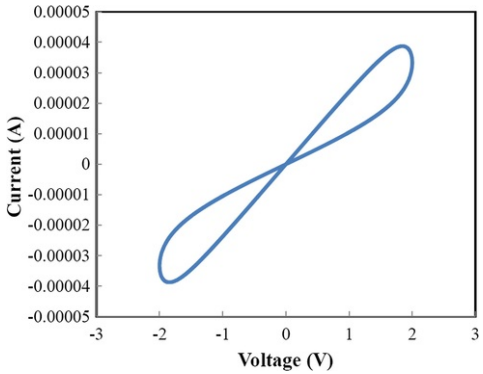

Fig. 20 The nonlinear *I-V* characteristic of the proposed window function for the frequency $f = 0.05$ Hz, $p = 2$, $U = \pm 2$ V and, $J = 1$.

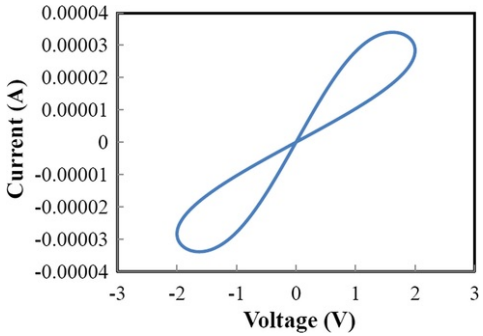

Fig. 21 Current-voltage response of the Proposed model for the $f = 2$ Hz, $p = 4$, $U = \pm 2$ V and, $J = 10$.

The reason being is that, for any higher values of p and J our proposed window function does not fix the values of $f(x)$ to any particular integer constant unlike other window functions known hitherto.

3.5.4 Threshold voltage controlled drift velocity (TVDV) model

Our proposed model also produces the Asymmetric Pinched Hysteresis Loop (APHL), which is achieved by threshold voltage controlled drift velocity of ions $(\frac{dw(t)}{dt})$ as shown in Eq. (9).

$$\frac{dw(t)}{dt} = \begin{cases} \frac{u_v R_{on} I(t)}{D} \cdot f(x) & V(t) \geqslant V_{on} \\ \frac{u_v R_{on} I(t)}{D} \cdot f(x) & V(t) \leqslant -V_{off} \\ \frac{u_v R_{on} I(t)}{D} \cdot f(x) & -V_{off} < V(t) < V_{on} \end{cases} \tag{9}$$

where V_{on} is the on-threshold voltage, V_{off} is the off-threshold voltage, $V(t)$ is the applied voltage, $I(t)$ is the current flow through the memristor, u_v is the mobility of ions, D is the distance between the two platinum electrodes.

Due to the existence of threshold voltages, drift velocity of ions increases/decreases nonlinearly based on the polarity of applied voltage. Correspondingly, memristance and width of the doped region increases/decreases nonlinearly. As a result, our model produces the APHL.

Fig. 22 illustrate the APHL which occurs during negative bias (reset process). Because, off-threshold voltage decreases the width movement speed. As a result, memristance increases and current conductivity decreases slowly. Thus our model produces APHL as well.

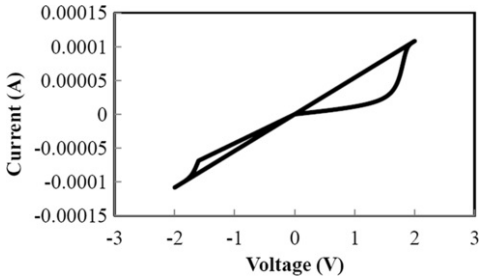

Fig. 22 Asymmetric current-voltage response of the proposed memristor model for $x = 0.5$, $p = 4$, $J = 10$, $V_{on} = 0.4$ and $V_{off} = -1.6$.

Fig. 23 also illustrates the APHL with large sized loop for the lower state variable and on/off threshold voltage. In general, it is known that nonlinearity is related to threshold voltage and loop size is related to state variable. If the value of state variable is low then the ionic drift increases/decreases slowly based on the polarity of applied voltage in turn affecting the width movement and current flow. These properties are responsible for obtaining large sized APHL in our memristor model.

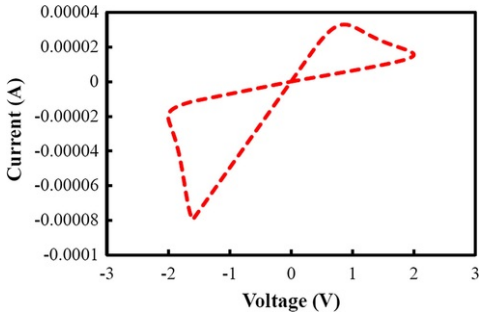

Fig. 23 Asymmetric current-voltage response of the proposed memristor model for $x = 0.2$, $p = 4$, $J = 10$, $V_{on} = 0.4$ and $V_{off} = -1.6$.

Interestingly, our proposed model corroborates with the observed property of physical memristor device ($Pt/TiO_{2-x}/TiO_2/Pt$) fabricated and studied in our lab [18]. The geometric parameters of the physical memristor used in the present study for comparison is for the thickness of bilayer is 147 nm, amplitude of the applied voltage is ±4 V and the frequency is 10 Hz as shown in Fig. 24.

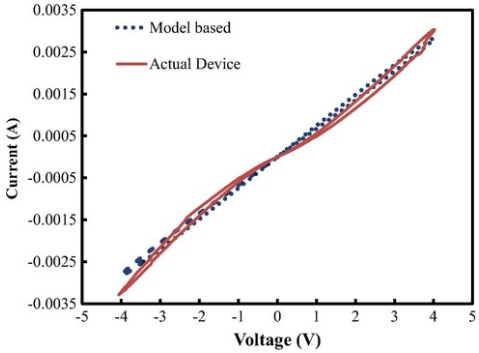

Fig. 24 Comparison of *I-V* curves obtained from the fabricated $Pt/TiO_{2-x}/TiO_2/Pt$ memristor device [18] with our proposed model (LIMM incorporating our new window function).

4 Results and discussions

In LIMM, ionic drift is considered to be linear. Therefore, the model does not mimic the properties of the physical memristor device as such. Hence, we are certain that the model requires a window function.

The Jogelker, Biolek and Prodromakis are the different types of window functions. In these window functions, it is understood that the nonlinearity and scalability are found to be very less. Therefore, a novel window function is required for the linear ion drift memristor model.

In the proposed window function the nonlinearity and scalability are very high compared to other window functions. The comparison results are shown in Table 1.

Table 1 A comparison of performance factors for different window functions.

Performance factors	Window functions						
	Jogelker	Biolek	Prodromakis	Fuzzy [16]	Sigmoidal [17]	Jinxiang* et al.	Proposed
Resolve Boundary effect	Yes	Yes	Yes	Yes	Yes	Yes	Yes
Scalability	No	Limited	Moderate	Yes	–	Yes	Yes
Control parameters	No	No	Yes	No	Yes	Yes	Yes
Nonlinearity	Limited	Yes	Yes	Yes	Yes	Yes	Yes

Asymmetric switching	No	No	No	Yes	No	No	Yes
Threshold Voltage	No	No	No	Yes	No	No	Yes
Resolve Boundary lock (Higher Voltage)	Limited	Limited	Moderate	Moderate	–	Moderate	Yes
Resolve Boundary lock (Lower Frequency)	No	No	No	–	–	No	Yes

– Not available.

*Jinxiang et al., window function is simulated and the results are tabulated.

In Jogelker and Biolek, for very small value of p, $f(x)$ value is fixed to one. Therefore, non-linearity and scalability are very limited. In Prodromakis, nonlinearity and controllability is moderate. But, the model does not produce the PHL for $p = 2$, $J = 1$, and $f < 0.1$ Hz. In Jinxiang et al., resolving the boundary lock problem (higher voltage) is moderate and the model does not produce the PHL for $p = 2$, $J = 1$, and $f = 0.05$ Hz. Therefore, this model fails to use in all the applications. Hence, the linear ion drift memristor model required a versatile window function to accommodate the observed setbacks as described above.

Thus, our proposed window function overcomes all the problems with high nonlinearity as the proposed window function is defined based on the cubic parabola and therefore, $f(x)$ value does not fix to any particular value producing the PHL for $f < 0.1$ Hz.

4.1 Application in an operational amplifier

In order to validate our claim, we have used our new model in an operational amplifier (op-amp) and demonstrating the amplification with high gain. Thus, we have used the memristor model incorporating the new window function and the functionality of memristor augmented Op-amp has been tested successfully. Fig. 25 shows the hybrid op-amp circuit (memristor/CMOS gates) consisting of CMOS based differential amplifier with memristor circuit topology. This circuit produces a high gain with low power dissipation compared to CMOS based operational amplifier as shown in Table 2 and its corresponding frequency response is illustrated in Fig. 26.

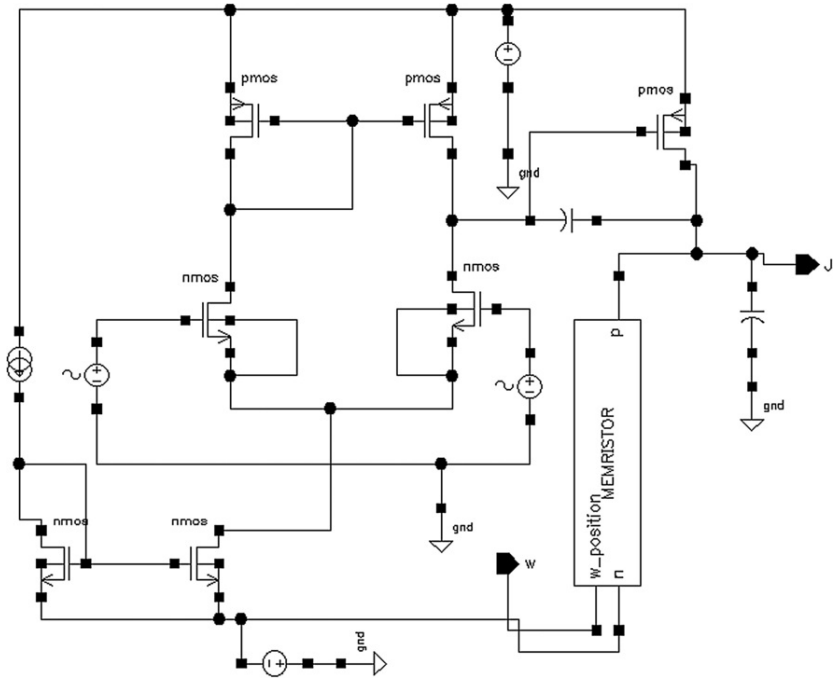

Fig. 25 Memristor based operational amplifier internal circuit topology.

Table 2 Comparison of results between CMOS and memristor based operational amplifier.

Op-amp	Power dissipation (μW)	GAIN (dB)
CMOS	745.93	62.144
Hybrid (CMOS and Memristor)	263.85	66.267

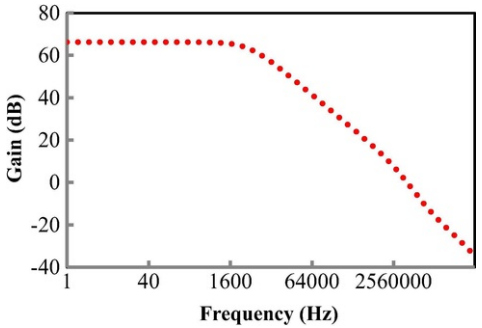

Fig. 26 Frequency response of a memristor based operational amplifier.

In a memristor based operational amplifier, our proposed model produces a high gain compared to other memristor models as shown in Table 3.

Table 3 Comparison results between different window functions and proposed memristor model.

Window functions	Gain (dB)
Jogelker	57.075
Biolek	7.85
Prodromakis	65.089
Jinxiang et al.	64.659
Proposed	66.267

5 Conclusion

The validation of our proposed model is carried out in Cadence® software, Virtuoso 6.0 tool. Interestingly, our proposed window function increases the nonlinearity and scalability in linear ion drift memristor model very significantly as compared to different existing models. Therefore, our proposed model mimics the properties of physical memristor device as exemplified. The main significance of our proposed model is that it retain~~ing~~s the PHL for higher voltages ~~and~~ as well as lower frequencies and also by adjusting the fitting parameters of window function. Hence, our model can be used in different memristor related applications with high performances.

Acknowledgment

~~Authors are indebted to the VIT management for extending the simulation facilities to carry out this work.~~ One of us (TAA) thanks VIT ~~the~~ management, Chennai for awarding ~~the~~ teaching assistantship.

Appendix A. Supplementary material

Supplementary data associated with this article can be found, in the online version, at https://doi.org/10.1016/j.aeue.2018.04.020.

References

[1] L.O. Chua, Memristor – the missing circuit element, *IEEE Trans Circuit Theory* **18** (5), 1971, 507–519.

[2] Dmitri B. Strukov, Gregory S. Snider, Duncan R. Stewart and R. Stanley Williams, The missing memristor found, *Nature* **453**, 2008, 80–83.

[3] Umut Engin Ayten, Shahram Minaei and S. Mehmet, Memristor emulator circuits using single CBTA, *Int J Electron Commun (AEÜ)* **82**, 2017, 109–118.

[4] C. Sánchez-López, M.A. Carrasco-Aguilar and Muniz-Montero, A 16 Hz–160 kHz memristor emulator circuit, *Int J Electron Commun (AEÜ)* **69**, 2015, 1208–1219.

[5] C. Sánchez-López and L.E. Aguila-Cuapio, A 860 kHz grounded memristor emulator circuit, *Int J Electron Commun (AEÜ)* **73**, 2017, 23–33.

[6] Mahdi. Tarkhan and Mohammad Maymandi-Nejad, Design of a memristor based fuzzy processor, *Int J Electron Commun (AEÜ)* **84**, 2018, 331–341.

[7] Joshua YangJ, Matthew D. Pickett, Xuema Li, Douglas A.A. Ohlberg, Duncan R. Stewart and R. Stanley Williams, Memristive switching mechanism for metal/oxide/metal nanodevices, *Nat Nanotechnol* **3**, 2008, 429–433.

[8] Matthew D. Pickett, Dmitri B. Strukov, Julien L. Borghetti, J. Joshua Yang, Gregory S. Snider, Duncan R. Stewart and R. Stanley Williams, Switching dynamics in titanium dioxide memristive devices, *J Appl Phys* **106**, 2009, 0745081–0745086.

[9] Shahar Kvatinsky, G. Friedman Eby, Avinoam Kolodny and C. WeiserUri, TEAM: threshold adaptive memristor model, *IEEE Trans Circuits Syst.-I* **60** (1), 2013, 211–221.

[10] Y.N. Jogelker and S.J. Wolf, The elusive memristor: properties of basic electrical circuits, *Eur J Phys* **30**, 2008, 661–675.

[11] Z. Biolek, D. Biolek and V. Biolkova, SPICE model of memristor with nonlinear dopant drift, *Radioengineering* **18** (2), 2009, 210–214.

[12] Themistoklis Prodromakis, Boon Pin Peh, Christos Papavassiliou and Christofer Toumazou, A versatile memristor model with nonlinear dopant kinetics, *IEEE Trans Electron Devices* **58** (9), 2011, 3099–3105.

[13] R. Williams, How we found the missing memristor, *IEEE Spectr* **45** (12), 2008, 28–35.

[14] Hu SG, Wu SY, Jia WW, Yu Q, Deng LJ, Fu YQ, et al. Review of nanostructured resistive switching memristor and its applications. Am Sci Publ, Nanosci Nanotechnol Lett 2014; 6(9): p. 729–757.

[15] Jinxiang Zha, He Huang and Yujie Liu, A novel window function for memristor model with application in programming analog circuits, *IEEE Trans Circuits Syst—ii: Express Briefs* **63** (5), 2016, 423–427.

[16] Rabab Farouk Abdel-Kader and Sherif M. Abuelenin, Memristor model based on fuzzy window function, *IEEE, Fuzzy Systems* 2015.

[17] P.S. Georgiou, S.N. Yaliraki, E.M. Drakakis and M. Barahona, Window functions and Sigmoidal behavior of memristive systems, *Int J Circ Theor Appl* **44** (9), 2016, 1685–1696.

[18] Satyajeet Sahoo, P. Manoravi P, S.R.S. Prabaharan SRS. Nano-ionic memristive crossbar architecture- fabrication, structure, surface properties and switching characteristics. Vacuum 2018 (Communicated).

Appendix A. Supplementary material

Multimedia Component 1

Supplementary data 1

Queries and Answers

Query: Your article is registered as a regular item and is being processed for inclusion in a regular issue of the journal. If this is NOT correct and your article belongs to a Special Issue/Collection please contact s.jayan@elsevier.com immediately prior to returning your corrections.
Answer: Yes

Query: The author names have been tagged as given names and surnames (surnames are highlighted in teal color). Please confirm if they have been identified correctly.
Answer: Yes. It is correctly identified